Published in final edited form as:
Cell Cycle. 2010 April 15; 9(8): 1639–1646.

Trypanosoma cruzi infection results in the reduced expression of caveolin-3 in the heart

Daniel Adesse[1,2,4], **Michael P. Lisanti**[6,7,*], **David C. Spray**[3,4], **Fabiana S. Machado**[5], **Maria de Nazareth Meirelles**[1], **Herbert B. Tanowitz**[2,3,*], and **Luciana Ribeiro Garzoni**[1]

[1]Laboratório de Ultra-Estrutura Celular; Instituto Oswaldo Cruz/FIOCRUZ; Rio de Janeiro, Brazil

[2]Department of Pathology, Albert Einstein College of Medicine; Bronx, NY USA

[3]Department of Medicine, Albert Einstein College of Medicine; Bronx, NY USA

[4]Dominick Purpura Department of Neuroscience; Albert Einstein College of Medicine; Bronx, NY USA

[5]Department of Biochemistry and Immunology; Institute of Biological Sciences; Federal University of Mina Gerais; Belo Horizonte, Brazil

[6]Department of Stem Cell Biology & Regenerative Medicine and the Kimmel Cancer Center; Thomas Jefferson University; Philadelphia, PA USA

[7]The Muscular and Neurodegenerative Disease Unit; University of Genoa and G. Gaslini Pediatric Institute; Genoa, Italy

Abstract

Caveolae are motile, membrane-bound compartments that contain a number of molecules that participate in cell signaling. Caveolins are protein markers of caveolae and function in a variety of biological processes. Caveolin-3 (Cav-3) is expressed in muscle cells and Cav-3 null mice display a cardiomyopathic phenotype. Ultrastructural cytochemistry, confocal microscopy and immunoblotting revealed a reduction in Cav-3 expression and an activation of ERK (extracellular-signal-regulated kinase) 48 hours after *Trypanosoma cruzi* infection of cultured cardiac myocytes. CD-1 mice infected with the Brazil strain of *T. cruzi* displayed reduced expression of Cav-3 and activation of ERK 66 days post infection (dpi). By 180 dpi there was a normalization of these values. These data suggest that the reduction in Cav-3 expression and the activation of ERK during the early phase of infection may contribute to the pathogenesis of chagasic cardiomyopathy.

Keywords

Trypanosoma cruzi; cardiac myocytes; caveolin-3; caveolae; ERK

Introduction

Chagas disease is caused by the protozoan parasite *Trypanosoma cruzi*,1 and results in heart disease in endemic areas of Latin America.2 Acute infection is usually associated with intense myocardial inflammation characterized by an upregulation of cytokines and

*Correspondence to: Michael P. Lisanti and Herbert B. Tanowitz; michael.lisanti@kimmelcancercenter.org and herbert.tanowitz@einstein.yu.edu.

chemokines.3,4 The ensuing cardiovascular remodeling may result in cardiomyopathy. The dilated cardiomyopathy is associated with congestive heart failure, arrhythmias, conduction abnormalities and thrombo-embolic events.2,5 The mouse model of *T. cruzi* infection has been intensely studied because it recapitulates many of the pathological, functional and immunological features of the human disease. In addition, primary cultures of rodent neonatal cardiac myocytes have been utilized as a tool to investigate the effect of *T. cruzi* on the heart.6–13 For example, *T. cruzi* alters cardiac myocyte Ca^{2+} homeostasis.6–13 and gap junctional communication.14,15 These infection-associated changes may contribute to the arrhythmias observed in this infection.

Caveolae are motile, membrane-bound compartments containing molecules that participate in cell signaling such as enzymes that generate messengers from substrates in the environment, substrates that are enzymatically converted into messengers and high-affinity binding sites that concentrate chemical signals. Caveolins are protein components of caveolae that are important in modulating a variety of biological functions including the modifications of signaling systems.18 Caveolae and caveolins play critical roles in calcium homeostasis in the heart16 and are disrupted by *T. cruzi* infection.17

Caveolae are signaling platforms that compartmentalize and concentrate signaling molecules such as G-protein subunits and endothelial nitric oxide synthase. Caveolins inhibit the downstream activation and signaling of many proteins, including c-Src, H-Ras, mitogen-activated protein (MAP) kinases, and eNOS.19,20 Caveolin-1 (Cav-1) is expressed ubiquitously, although at different levels in different tissues; Cav-2 is tightly co-expressed with Cav-1, whereas Cav-3 is expressed predominantly in striated muscle cells.21 Importantly, Cav-1 and Cav-3 null mice display a cardiomyopathy, with left ventricle wall thickening, fibrosis and p42/44 MAPK (ERK 1/2) activation.22

The activation of ERK1/2 plays an important role in the pathogenesis of cardiac hypertrophic responses and cellular proliferation in the cardiovascular system.23 In vitro data support a role for Cav-1 and Cav-3 as negative regulators of ERK signaling.24 During acute infection with the Tulahuen strain of *T. cruzi* Nagajyothi et al.17 described reduced levels of Cav-1, -2 and -3 and increased ERK phosphorylation in hearts from infected mice. *T. cruzi* infection of mice and of cultured endothelial and smooth muscle cells resulted in activation of AP-1 which participates in cardiovascular remodeling through ERK 1/2 phosphorylation.25,26

We now report that the infection of cultured cardiac myocytes with *T. cruzi* resulted in a reduction of Cav-3 expression and activation of ERK 1/2. This was also observed in infected mice. These observations strongly suggest that infection with *T. cruzi* results in the reduced expression of Cav-3 and the activation of ERK. The cardiomyopathic phenotype of Cav-3 null mice suggests that a reduction in Cav-3 expression contributes to the cardiomyopathy of chagasic cardiomyopathy. ERK likely plays an important role in cardiac remodeling and arrhythmogenesis that accompany chagasic cardiomyopathy.

Results

Caveolae and caveolin-3 (Cav-3) expression are reduced as a result of *T. cruzi* infection

Ultrastructural analysis revealed that uninfected cardiac myocytes displayed features of differentiated myocytes such as myofibrils near mitochondria, sarcoplasmic reticulum, T-tubules and cell-cell junctions (Fig. 1A–C). Use of the lanthanum (La) as an electron opaque tracer for divalent ion (Ca^{2+}) binding sites revealed numerous caveolae on the surface of cultured cardiac myocytes and subsurface vesicles containing the tracer (Fig. 1B and C). After 24 hours of infection, trypomastigotes were identified by the presence of basket

shaped kinetoplasts and subpellicular microtubules (Fig. 1D). We observed intracellular amastigotes in the cytoplasm of host cells presenting typical structures such as reservosomes and acidocalcisomes at 48 h (Fig. 1E). Beginning at 24 hr post infection, there was both reduced surface staining with La and a smaller number of caveolae in infected cells (Fig. 1D). These differences persisted at longer time-points, with surface La labeling virtually absent at 72 hours post infection (Fig. 1E and F).

To quantitate alterations in caveolae and Cav-3 abundance and distribution, we performed immunostaining and immunoblotting during the course of infection. Cultured cardiac myocytes displayed specific reactivity to anti-Cav-3 antibody, since no staining was detected in endothelial cells or fibroblasts (not shown). Cav-3 expression was abundant at and beneath the surface membrane of cardiac myocytes cultured for 96 hours (Fig. 2). However, 72 hours post infection, highly infected cells showed a striking reduction in Cav-3 immunoreactivity (Fig. 2B). Immunoblot analyses of the myocytes were consistent with both La cytochemistry and Cav-3 immunostaining. We observed that infected cardiac myocytes displayed Cav-3 levels similar to controls at 24 hours post infection and that there was a significant reduction at 48 (74%) and 72 (51%) hours post infection ($p < 0,05$, ANOVA) (Fig. 2C and D).

T. cruzi in vivo infection and caveolin-3 (Cav-3) expression

We further analyzed the changes in Cav-3 in infected mice 66 and 180 days post infection (dpi). Immunoblot analysis of the heart tissue at these time points revealed that at 66 dpi there was a 46% decrease in Cav-3 levels, which were fully restored at 180 dpi (Fig. 3). Immunohistochemistry of the heart tissue at 66 dpi revealed that non-infected animals displayed abundant Cav-3 amongst cardiac myocytes, with T-tubule patterns (Fig. 3 and arrows). This pattern was altered in infected hearts, where we observed areas of tissue damage (Fig. 3B) and areas in which cardiac myocytes displayed mostly intracellular staining.

T. cruzi and ERK phosphorylation

Since an inverse relationship has been reported between the activation of ERK and the reduction in Cav-3 expression24 we examined the impact of infection on ERK activation in cardiac myocytes at various time-points post infection, from one to 72 hours. The protein lysates were subjected to immunoblot analysis and probed with specific antibodies. We verified that at all time points studied, the infection did not alter total ERK expression (Fig. 4A and B). However, there was a progressive activation of ERK, as evidenced by increased phosphorylation in the cardiac myocytes; starting at 2 hours post infection (40%) and a 3-fold increase 72 hours post infection (Fig. 4A and B). We next analyzed ERK expression activation in hearts of infected mice at 66 and 180 dpi. While total ERK expression remained unaltered, phosphorylated forms of ERK at 66 dpi (when Cav-3 levels were decreased) had a 2.3-fold increase when compared to age-matched controls. At 180 dpi we observed that phosphoERK expression was 68% decreased in infected heart tissue (Fig. 4C and D).

Discussion

The effects of *T. cruzi* infection and its progression to heart disease is an ongoing interest by our groups and of others, since chagasic cardiomyopathy is the main cause of heart disease in Latin America. The parasite alters many of the host cell processes such as intracellular calcium homeostasis,9,27 cell-cell communication14,15 and cytoskeleton stability.28,29 Alterations caused to host cells in the heart during acute infection where tissue parasitism is

high and is associated with an intense inflammatory response and myonecrosis, may determine the development of the chronic disease.

In the present study, we have focused on caveolae, which are membrane-bound signaling complexes involved in Ca^{2+} homeostasis as well as other cell functions.19 We evaluated the distribution of caveolae on infected cardiac myocytes by ultra-structural cytochemistry using lanthanum nitrate (La). La displaces Ca^{2+} from its binding sites on sarcolemma and can be used as a tracer for surface Ca^{2+} binding sites, abundantly found in caveolae.30,31 The La staining permits the observation of caveolae distribution and intracellular vesicles, with positive La staining indicating sites of transport and storage of Ca^{2+}. In the current study we observed that *T. cruzi*-infected cardiac myocytes displayed a reduction in La staining on sarcolemma when compared with non infected cells after 48 hours of infection.32 This is in agreement with previous results showing (a) that *T. cruzi* could alter cardiac myocyte endocytotic uptake of small molecules,32 and (b) that caveolin (Cav)-1 null mice also display impaired endocytosis. 33 We confirmed the alterations in caveolae distribution during infection with *T. cruzi* by immunostaining and immunblot analysis demonstrating a significant reduction in the expression of Cav-3 48 and 72 hours post infection. Since caveolae are involved in Ca^{2+} regulation in cardiac myocytes and *T. cruzi* infection alters these structures, it is possible that caveolae disruption could be involved with the changes on Ca^{2+} homeostasis in cardiac myocytes. By depleting caveolae with cyclodextrin34, a dose-dependent decrease in frequency, amplitude and spatial extent of Ca^{2+} sparks was observed in smooth muscle cells and in cardiac myocytes. These observations suggest that alterations in the molecular assembly and ultra-structure of caveolae may lead to pathophysiological changes in Ca^{2+} signaling. Through disruption of Ca^{2+} homeostasis, alteration in caveolae may contribute to the occurrence of arrhythmias observed in chagasic heart disease.

One major mechanism by which expression of caveolins is downregulated is activation of the mitogen-activated protein kinase family (MAPK), including the p42/44 MAPK, also known as extracellular signal regulated kinase (ERK 1/2).19,35 The infected myocytes displayed activation of this protein kinase starting at two hours post infection as determined by immunoblot analysis using phospho-specific antibodies, without any significant alteration in total protein expression. This observation is consistent with our previous demonstration of ERK activation in cultured endothelial and smooth muscle cells after infection with the Tulahuen strain of *T. cruzi*.25

Since ERK phosphorylation is involved in cardiac remodeling, we studied Cav-3 and phospho-ERK expression in heart lysates of infected mice 66 days and 180 days post infection. Cav-3 levels were drastically reduced at 66 dpi as observed by immunohistochemistry and immunoblot; and a three-fold increase in ERK phosphorylation was observed. This in accordance with previous studies that shown reduced Cav-1, Cav-2 and Cav-3 during acute murine *T. cruzi* infection followed by ERK phosphorylation.3,17 Cav-1 null mice display hyperactivation of ERK in the heart and these mice also display cardiac hypertrophy with normal substrate utilization and expression of genes involved in energy metabolism. 36–38 In addition, Cav-3 null mice display increased expression of phosphorylated ERK and a cardiomyopathic phenotype.22

The observations in the current report demonstrate that *T. cruzi* infection alters Cav-3 expression in cardiac myocytes. The ERK 1/2 activation indicates that Cav-3 downregulation an important contributor in the cardiac injury observed during chagasic cardiomyopathy, including the hypertrophy, inflammation, fibrosis and arrhythmias, as observed in Cav-1, Cav-3 and the double knockout mice.22,36,37 These observations also suggest that the caveolins may provide a novel target for potential therapeutic agents.

Material and Methods

Parasites and mice

The Brazil strain of *T. cruzi* was maintained in C3H/Hej (Jackson Laboratories, Bar Harbor, ME) mice. For mouse experiments 6–8 week old male CD-1 mice were injected with 5×10^4 trypomastigotes of the Brazil strain and parasitemia was evaluated by counting in a hemocytometer. All experiments were approved by the Institutional Animal Care Committee of the Albert Einstein College of Medicine. For in vitro experiments the Y strain was utilized. These trypomastigotes were maintained in cultured cardiac myocytes as previously described until used.39

CD-1 mice infected with the Brazil strain had a mortality of 50% by 45 days post infection (dpi). The parasitemia peaked at 30 to 35 dpi at 7.5×10^5 trypomastigotes/ml and then waned. There was no mortality after 45 dpi. Hearts were collected at 66 dpi and 180 dpi. Samples were either processed for immunohistochemistry or quick frozen in liquid nitrogen, crushed using a mortar and pestle (Humboldt, Schiller Park, IL), resuspended in lysis buffer and sonicated for immunoblotting.

Reagents and antibodies

Trypsin was obtained from Difco Laboratories (Detroit, Michigan), Type II collagenase was obtained from Worthington Biochemical Corporation (Lakewood, NJ). Fetal bovine serum (FBS), L-glutamine, penicillin, streptomycin, $CaCl_2$, Dulbecco's Modified Eagle's Medium (DMEM), RPMI, glutaraldehyde, sodium cacodylate, osmium tetroxide,acetoneand bovine serum albumin (BSA) were obtained from Sigma-Aldrich (St. Louis, MO). Lanthanum nitrate was obtained from Merk KGaA, (Darmstadt, Germany) and Epon 812 resin from Polysciences Inc., (Warrington, PA). Anti-caveolin-3 antibody was obtained from Affinity Bioreagents (Golden, CO), polyclonal goat anti-rabbit Alexa Fluor 488 antibody was obtained from Invitrogen (Carlsbad, CA), BCA Protein Assay Reagent (bicinchoninic acid) and 4'-6-Diamidino-2-phenylindole (DAPI) from Thermo Scientific (Rockford, IL). Rabbit polyclonal anti-phosphorylated ERK and total ERK were obtained from Cell Signaling (Beverly, MA) and the Protease Inhibitor Cocktail was obtained from Roche Molecular Biochemicals (Indianapolis, IN.) Goat anti-rabbit IgG and goat anti-mouse IgG HRP-labeled antibody were obtained from Santa Cruz Biotechnology (Santa Cruz, CA). Anti-BIP antibodies were obtained from Affinity Bioreagents (Rockford, IL).

Experiments with cardiac myocytes

Hearts were obtained from 18 day old embryos of mice and disassociated by mechanical and enzymatic dissociation methods using 0.05% trypsin and 0.01% collagenase in phosphate buffered saline (PBS, pH 7.2) at 37°C, following methods previously described.5 Briefly, ventricular heart muscle cells were plated on 0.02% gelatin-coated glass cover slips maintained in 24-well plates for immunostaining assays or on plastic dishes for electron microscopy and immunoblotting. The cells were maintained at 37°C in 5% CO_2 atmosphere in DMEM supplemented with 5% FBS, 1 mM $CaCl_2$, 1 mM L-glutamine, 2% chick embryo extract, 1,000 U/mL penicillin and streptomycin 50 $\mu g/ml^{-1}$ (complete Eagle medium). Cardiac myocytes were infected with the Y strain trypomastigotes at a multiplicity of infection of 10:1.

Ultra-structural cytochemistry

Uninfected and *T. cruzi*-infected cardiac myocytes cultured in plastic culture dishes were washed with PBS, fixed with 2.5% glutaraldehyde for 1 hour at 4°C, followed by washes first with Na-cacodylate buffer and then collidine buffer. Cells were post-fixed with 1% osmium tetroxide, 1.3% lanthanum nitrate in collidine buffer for 2 hours at 4°C. Cells were

then dehydrated in an ascending series of acetone (30–100%) and embedded in Epon 812 resin. Ultra-thin sections were picked up with 300-mesh copper grids, stained with uranyl acetate and lead citrate and examined using a Zeiss EM 10C transmission electron microscope.

Immunofluorescence

Cells were washed with PBS (pH 7.2) at 72 hours post infection and fixed in 4% paraformaldehyde for 5 minutes at 20°C. After the washes cells were permeabilized with 0.05% Triton and non-specific staining was blocked with 4% BSA. Anti-Cav-3 antibody was incubated overnight 4°C, after which cells were washed and incubated with secondary polyclonal goat anti-rabbit Alexa Fluor 488 antibody for 1 hour at 37°C. DNA was stained with DAPI. For immunohistochemistry of heart tissue sections, samples were embedded in paraffin, sectioned with a microtome and placed on slides. Paraffin was removed incubating slides at 60°C, then with xylene and descending ethanol series. After washes with PBS, samples were blocked with BSA and incubated with anti-caveolin-3 antibody for 72 hours at 4°C. Secondary anti-rabbit Alexa Fluor 488 antibody was incubated for 2 hours at 20°C. Auto-fluorescence of the heart tissue was removed by incubating samples with 0.01% Evans blue solution and DNA was stained with DAPI. All slides were mounted with DABCO and images were acquired with a Zeiss 510 Meta Laser Scanning Confocal Microscope.

Immunoblotting

At desired times, cells were washed three times with PBS and scraped with 300 µl of lysis buffer (2 mM PMSF, 5 mM EDTA, 1 mM Na_3 VO_4, 1 mM $NaHCO_3$, 10% Roche Protease Inhibitor Cocktail at 1, 2, 6, 24, 48 and 72 hours post infection). Hearts from infected CD1 mice and age-matched control mice were frozen in liquid nitrogen, resuspended in lysis buffer and sonicated. Samples were frozen at −80°C until used, the lysates were sonicated and protein concentration was measured using the BCA Protein Assay Reagent. Five to 10 µg of protein was loaded and resolved in 12% SDS-polyacrylamide gels. After resolving, proteins were transferred to nitrocellulose membranes (Whatman) and incubated with rabbit polyclonal anti-caveolin-3 antibody or rabbit polyclonal anti-phosphorylated ERK or total ERK diluted in TBST with 5% skim milk overnight at 4°C. For loading controls mouse anti-Glyceraldehyde 3-phosphate dehydrogenase (GAPDH, 36 KDa) monoclonal antibody and anti-BIP antibody were used. Membranes were washed with TBST and incubated with secondary goat anti-rabbit IgG and secondary goat anti-mouse IgG HRP-labeled antibody for 1 h at 25°C, followed by incubation with chemoluminescent kit ECL.

Statistical analysis

Statistical analyses were performed using the ANOVA test, with the level of significance set at $p < 0.05$. The data represent average (±standard error of the mean) and a minimum of three independent experiments.

Acknowledgments

PAPES (Programa de Apoio a Pesquisa-CNPq); D.A. was supported in part by a Fogarty International Training Grant D43 TW007129 (H.B.T.). This work was also supported by NIH grants AI076248 and AI052739 (H.B.T.) and HL-73732 (H.B.T. and D.C.S.) and by CNPq (M.N.M.) and FAPEMIG and PRPq-UFMG (F.S.M.). The authors thank Ms. Angela Santos and Mr. Dazhi Zhao for the excellent technical support.

References

1. Chagas C. Nova espécie morbida do homem, produzida por um Trypanosoma (*Trypanosoma cruzi*): Nota prévia, Brasil Médico. 1909; 23:161.

2. Tanowitz HB, Machado FS, Jelicks LA, Shirani J, de Carvalho AC, Spray DC, et al. Perspectives on *Trypanosoma cruzi*-induced heart disease (Chagas disease). Prog Cardiovasc Dis. 2009; 51:524–539. [PubMed: 19410685]
3. Huang H, Chan J, Wittner M, Jelicks LA, Morris SA, Factor SM, et al. Expression of cardiac cytokines and inducible form of nitric oxide synthase (NOS2) in *Trypanosoma cruzi*-infected mice. J Mol Cell Cardiol. 1999; 31:75–88. [PubMed: 10072717]
4. Machado FS, Souto JT, Rossi MA, Esper L, Tanowitz HB, Aliberti J, et al. Nitric oxide synthase-2 modulates chemokine production by *Trypanosoma cruzi*-infected cardiac myocytes. Microbes Infect. 2008; 10:1558–1566. [PubMed: 18951994]
5. Punukollu G, Gowda RM, Khan IA, Navarro VS, Vasavada BC. Clinical aspects of the Chagas' heart disease. Int J Cardiol. 2006; 115:279–283. [PubMed: 16769134]
6. Meirelles MN, de Araujo-Jorge TC, Miranda CF, de Souza W, Barbosa HS. Interaction of *Trypanosoma cruzi* with heart muscle cells: ultra-structural and cytochemical analysis of endocytic vacuole formation and effect upon myogenesis in vitro. Eur J Cell Biol. 1986; 41:198–206. [PubMed: 3093234]
7. Aprigliano O, Masuda MO, Meirelles MN, Pereira MC, Barbosa HS, Barbosa JC. Heart muscle cells acutely infected with *Trypanosoma cruzi*: characterization of electrophysiology and neurotransmitter responses. J Mol Cell Cardiol. 1993; 25:1265–1274. [PubMed: 8263957]
8. Barbosa HS, Meirelles MN. Evidence of participation of cytoskeleton of heart muscle cells during the invasion of *Trypanosoma cruzi*. Cell Struct Funct. 1995; 20:275–284. [PubMed: 8521528]
9. Garzoni LR, Masuda MO, Capella MM, Lopes AG, de Meirelles Mde N. Characterization of $[Ca^{2+}]_i$ responses in primary cultures of mouse cardiomyocytes induced by *Trypanosoma cruzi* trypomastigotes. Mem Inst Oswaldo Cruz. 2003; 98:487–493. [PubMed: 12937759]
10. Taniwaki NN, Machado FS, Massensini AR, Mortara RA. *Trypanosoma cruzi* disrupts myofibrillar organization and intracellular calcium levels in mouse neonatal cardiomyocytes. Cell Tissue Res. 2006; 324:489–496. [PubMed: 16501996]
11. Moreno SN, Silva J, Vercesi AE, Docampo R. Cytosolic-free calcium elevation in *Trypanosoma cruzi* is required for cell invasion. J Exp Med. 1994; 180:1535–1540. [PubMed: 7931085]
12. Rodriguez A, Rioult MG, Ora A, Andrews NW. A trypanosome-soluble factor induces IP3 formation, intracellular Ca^{2+} mobilization and microfilament rearrangement in host cells. J Cell Biol. 1995; 129:1263–1273. [PubMed: 7775573]
13. Bergdolt BA, Tanowitz HB, Wittner M, Morris SA, Bilezikian JP, Moreno AP, et al. *Trypanosoma cruzi*: effects of infection on receptor-mediated chronotropy and Ca^{2+} mobilization in rat cardiac myocytes. Exp Parasitol. 1994; 78:149–160. [PubMed: 8119371]
14. de Carvalho AC, Tanowitz HB, Wittner M, Dermietzel R, Roy C, Hertzberg EL, et al. Gap junction distribution is altered between cardiac myocytes infected with *Trypanosoma cruzi*. Circ Res. 1992; 70:733–742. [PubMed: 1551199]
15. Adesse D, Garzoni LR, Huang H, Tanowitz HB, de Nazareth Meirelles M, Spray DC. *Trypanosoma cruzi* induces changes in cardiac connexin43 expression. Microbes Infect. 2008; 10:21–28. [PubMed: 18068391]
16. Furstenau M, Lohn M, Ried C, Luft FC, Haller H, Gollasch M. Calcium sparks in human coronary artery smooth muscle cells resolved by confocal imaging. J Hypertens. 2000; 18:1215–1222. [PubMed: 10994752]
17. Nagajyothi F, Desruisseaux M, Bouzahzah B, Weiss LM, Andrade Ddos S, Factor SM, et al. Cyclin and caveolin expression in an acute model of murine Chagasic myocarditis. Cell Cycle. 2006; 5:107–112. [PubMed: 16319533]
18. Sargiacomo M, Sudol M, Tang Z, Lisanti MP. Signal transducing molecules and glycosyl-phosphatidylinositol-linked proteins form a caveolin-rich insoluble complex in MDCK cells. J Cell Biol. 1993; 122:789–807. [PubMed: 8349730]
19. Williams TM, Lisanti MP. The Caveolin genes: from cell biology to medicine. Ann Med. 2004; 36:584–595. [PubMed: 15768830]
20. Tourkina E, Richard M, Gööz P, Bonner M, Pannu J, Harley R, et al. Antifibrotic properties of caveolin-1 scaffolding domain in vitro and in vivo. Am J Physiol Lung Cell Mol Physiol. 2008; 294:843–861.

21. Song KS, Scherer PE, Tang Z, Okamoto T, Li S, Chafel M, et al. Expression of caveolin-3 in skeletal, cardiac and smooth muscle cells. Caveolin-3 is a component of the sarcolemma and co-fractionates with dystrophin and dystrophin-associated glycoproteins. J Biol Chem. 1996; 271:15160–15165. [PubMed: 8663016]
22. Woodman SE, Park DS, Cohen AW, Cheung MW, Chandra M, Shirani J, et al. Caveolin-3 knock-out mice develop a progressive cardiomyopathy and show hyperactivation of the p42/44 MAPK cascade. J Biol Chem. 2002; 277:38988–38997. [PubMed: 12138167]
23. Gillespie-Brown J, Fuller SJ, Bogoyevitch MA, Cowley S, Sugden PH. The mitogen-activated protein kinase kinase MEK1 stimulates a pattern of gene expression typical of the hypertrophic phenotype in rat ventricular cardiomyocytes. J Biol Chem. 1995; 270:28092–28096. [PubMed: 7499296]
24. Engelman JA, Chu C, Lin A, Jo H, Ikezu T, Okamoto T, et al. Caveolin-mediated regulation of signaling along the p42/44 MAP kinase cascade in vivo. A role for the caveolin-scaffolding domain. FEBS Lett. 1998; 428:205–211. [PubMed: 9654135]
25. Mukherjee S, Huang H, Petkova SB, Albanese C, Pestell RG, Braunstein VL, et al. *Trypanosoma cruzi* infection activates extracellular signal-regulated kinase in cultured endothelial and smooth muscle cells. Infect Immun. 2004; 72:5274–5282. [PubMed: 15322023]
26. Huang H, Petkova SB, Cohen AW, Bouzahzah B, Chan J, Zhou J-N, et al. Activation of transcription factors (AP-1 and NFκB) in murine chagasic myocarditis. Activation of transcription factors AP-1 and NFκB in murine *Chagasic myocarditis*. Infect Immun. 2003; 71:2859–2867. [PubMed: 12704159]
27. Tardieux I, Webster P, Ravesloot J, Boron W, Lunn JA, Heuser JE, et al. Lysosome recruitment and fusion are early events required for trypanosome invasion of mammalian cells. Cell. 1992; 71:1117–1130. [PubMed: 1473148]
28. Mott A, Lenormand G, Costales J, Fredberg JJ, Burleigh BA. Modulation of host cell mechanics by *Trypanosoma cruzi*. J Cell Physiol. 2009; 218:315–322. [PubMed: 18853412]
29. Pereira MC, Costa M, Chagas Filho C, de Meirelles MN. Myofibrillar breakdown and cytoskeletal alterations in heart muscle cells during invasion by *Trypanosoma cruzi*: immunological and ultrastructural study. J Submicrosc Cytol Pathol. 1993; 25:559–569. [PubMed: 8269403]
30. Langer GA, Frank JS. Lanthanum in heart cell culture. Effect on calcium exchange correlated with its localization. J Cell Biol. 1972; 54:441–455. [PubMed: 5044754]
31. Miller TW, Tormey JM. Calcium displacement by lanthanum in subcellular compartments of rat ventricular myocytes: characterization by electron probe microanalysis. Cardiovasc Res. 1993; 27:2106–2112. [PubMed: 8313415]
32. Soeiro MN, Silva-Filho FC, Meirelles MN. The nature of anionic sites and the endocytic pathway in heart muscle cells. J Submicrosc Cytol Pathol. 1994; 26:121–130. [PubMed: 8149329]
33. Li J, Scherl A, Medina F, Frank PG, Kitsis RN, Tanowitz HB, et al. Impaired phagocytosis in caveolin-1 deficient macrophages. Cell Cycle. 2005; 4:1599–1607. [PubMed: 16205123]
34. Lohn M, Furstenau M, Sagach V, Elger M, Schulze W, Luft FC, et al. Ignition of calcium sparks in arterial and cardiac muscle through caveolae. Circ Res. 2000; 87:1034–1039. [PubMed: 11090549]
35. Cohen AW, Hnasko R, Schubert W, Lisanti MP. Role of caveolae and caveolins in health and disease. Physiol Rev. 2004; 84:1341–1379. [PubMed: 15383654]
36. Park DS, Woodman SE, Schubert W, Cohen AW, Frank PG, Chandra M, et al. Caveolin-1/3 double-knockout mice are viable, but lack both muscle and non-muscle caveolae, and develop a severe cardiomyopathic phenotype. Am J Pathol. 2002; 160:2207–2217. [PubMed: 12057923]
37. Cohen AW, Park DS, Woodman SE, Williams TM, Chandra M, Shirani J, et al. Caveolin-1 null mice develop cardiac hypertrophy with hyperactivation of p42/44 MAP kinase in cardiac fibroblasts. Am J Physiol Cell Physiol. 2003; 284:457–474.
38. Augustus AS, Buchanan J, Gutman E, Rengo G, Pestell RG, Fortina P, et al. Hearts lacking caveolin-1 develop hypertrophy with normal cardiac substrate metabolism. Cell Cycle. 2008; 7:2509–2518. [PubMed: 18719368]

39. Garzoni LR, Caldera A, Meirelles Mde N, de Castro SL, Docampo R, Meints GA, et al. Selective in vitro effects of the farnesyl pyrophosphate synthase inhibitor risedronate on *Trypanosoma cruzi*. Int J Antimicrob Agents. 2004:23273–23285.

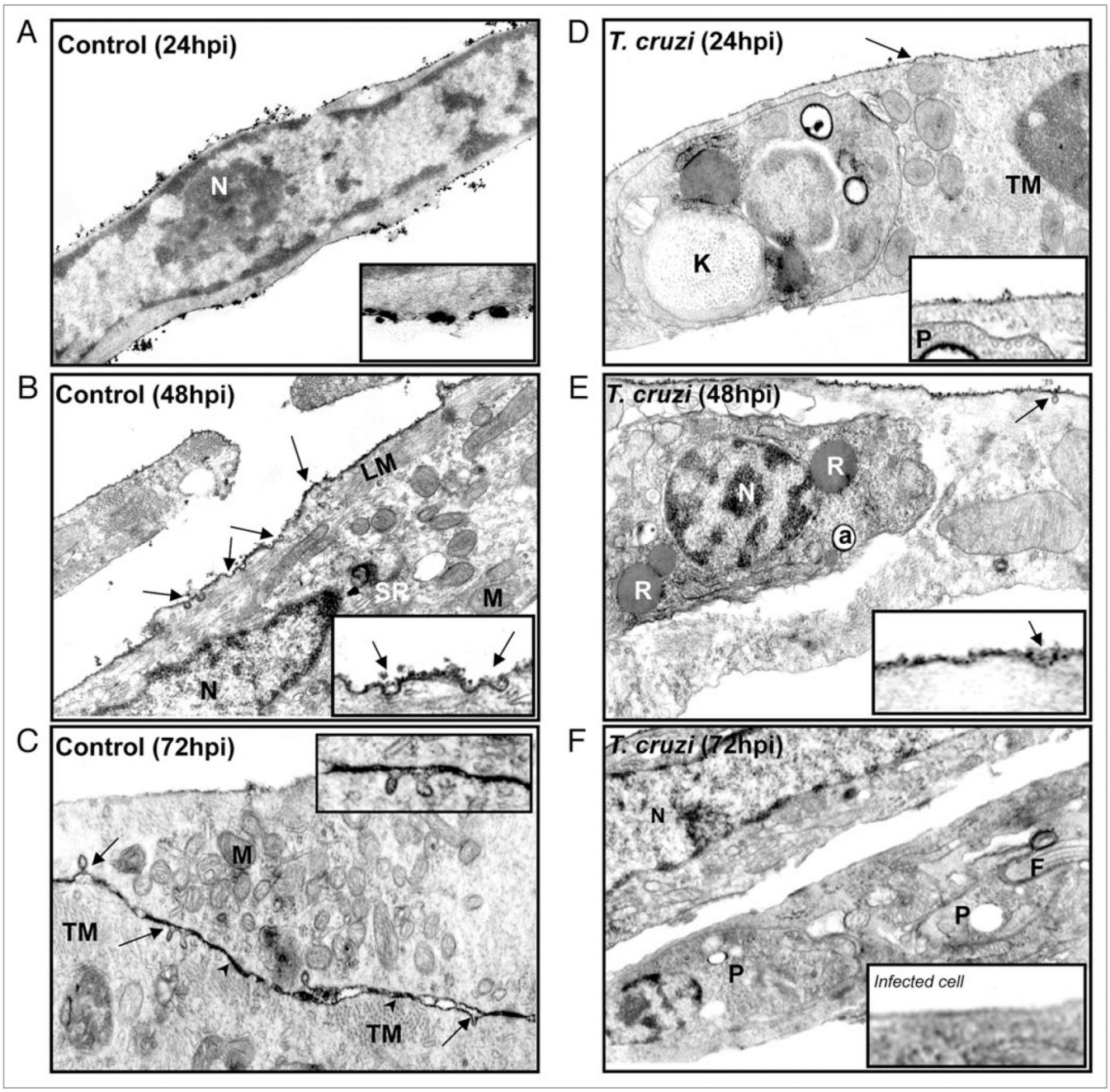

Figure 1.

Ultrastructural cytochemistry. The tracer Lanthanum (La) Nitrate was used to reveal Ca^{2+} binding sites in cardiac myocytes. (A–C) Representative uninfected cardiac myocytes displayed longitudinal (LM) and transversal (TM) myofibrils, abundant mitochondria (M) and T-tubules (TT). Note in (C) the cell-cell junctions are depicted by arrowheads. La staining reveals intense electron dense staining in the plasma membrane with many caveolae (arrows), which can be observed in more detail in the inserts. (C) Some vesicles close to the membrane show staining with the tracer. (D) After 24 hours of infection a parasite is observed with subpellicular microtubules and a round kinetoplast (K). (E) A representative infected cardiac myocyte 48 hours post infection containing an intracellular amastigote with

a reservosome (R) and an acidocalcisome (a). (N = Nucleus). (F) There was a reduction in La staining and alterations in caveolae abundance 72 hours after infection. Trypomastigotes (P) are observed in the cell cytoplasm and a decrease in surface staining by La. Original magnification: (A and F) = 26,000X; (B, C and E) = 41,000X; (D) = 47,350X.

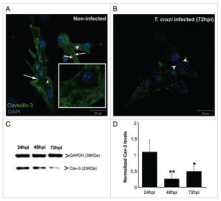

Figure 2.

Caveolin-3 (Cav-3) expression is decreased after *T. cruzi* infection. Cultured cardiac myocytes were infected for 3 days. (A) Representative confocal Laser Scanning analysis of Cav-3 distribution in uninfected cardiac myocytes fixed and stained after 96 hours in culture. Cells presented abundant caveosomes (arrowheads) and peripheral staining (white arrows). The inset depicts higher magnification of the Cav-3 staining. (B) After 72 hours of infection, Cav-3 signal was reduced among highly parasitized cardiac myocytes, present mostly at cell periphery and with reduced presence of caveosomes. (C) Representative immunoblot of Cav-3 (23 KDa) expression in infected and uninfected cardiac myocytes. Anti-GAPDH (36 KDa) antibody was used as a loading control. (D) Bar graph demonstrating quantification of Cav-3 expression as normalized by GAPDH. There was a significant decrease of Cav-3 expression 48 (74%) and 72 (51%) hours post infection (n = 4) $^{**}p < 0.01$; $^{*}p < 0.05$, ANOVA. Bars = 20 μm.

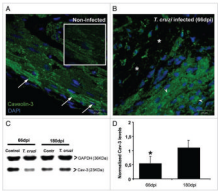

Figure 3.

Caveolin-3 (Cav-3) in infected hearts. Hearts obtained from infected (Brazil strain) and uninfected CD-1 mice were embedded in paraffin and processed for immunohistochemistry. Sections were stained with anti-Cav-3 antibody (green) and DAPI (blue) and observed by confocal microscopy. (A) Representative uninfected cardiac tissue displayed intense Cav-3 staining of cardiac myocytes, especially in pericardial area with T-tubule patterns (arrows). The inset shows higher magnification of the Cav-3 staining. (B) This staining pattern was altered in the hearts of infected mice at 66 days post infection (dpi) where areas of tissue damage were evident (*). In other areas Cav-3 staining was observed mainly in the cytoplasm of cardiac myocytes (arrowheads). Bars = 20 μm. (C) Representative immunoblot lot analysis of Cav-3 expression in cardiac tissue. Hearts of mice 66 and 180 dpi were harvested and protein lysates probed with anti-Cav-3 antibody. GAPDH (36 KDa) was used as a loading control. At 66 dpi, infection induced 46% reduction in Cav-3 expression, which was restored to control levels at 180 dpi (n = 4 for each group). (*$p < 0.05$, ANOVA).

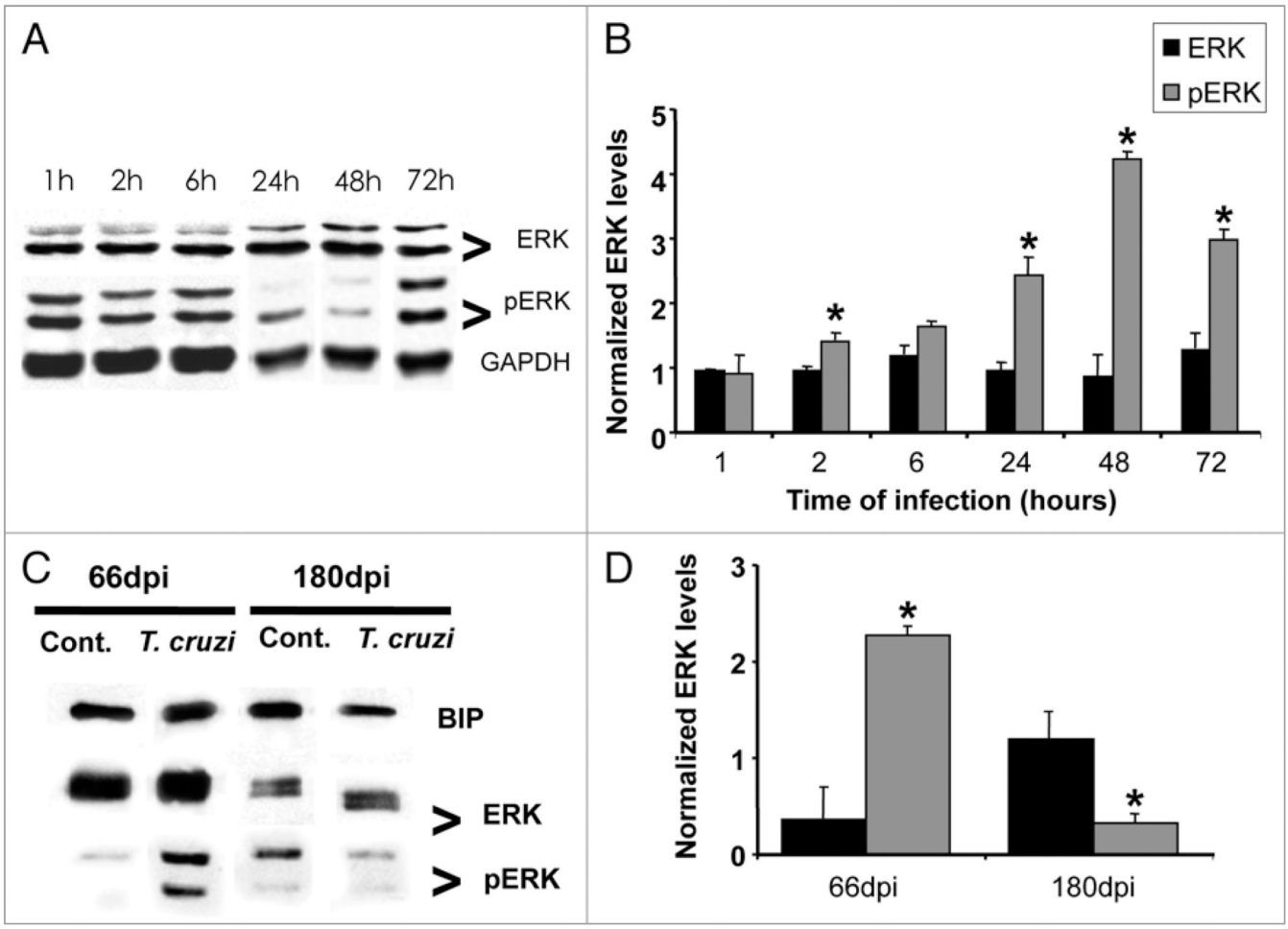

Figure 4.

Trypanosoma cruzi infection induces activation of ERK 1/2 in cultured cardiac myocytes and in the myocardium of infected mice. (A) Cultured cardiac myocytes were infected with *T. cruzi* and blots were probed against anti-total ERK and pERK. There was no change in total ERK over a 72 hours infection. However, a progressive increase in pERK (activation) over the same period of time was observed. GAPDH (36 KDa) was used as loading control in myocyte samples (n = 3 for each group). (C and D) Hearts obtained from Brazil strain infected mice (66 and 180 days post infection, dpi) were subjected to SDS-PAGE analysis and probed with anti-phosphoERK antibody. *T. cruzi* infection induced a 2.3-fold increase in pERK (activation) at 66 dpi and a 68% decrease at 180 dpi as compared with age-matched uninfected controls. BIP (78 KDa) was used as loading control for heart tissue samples (n = 4 for each group) (*$p < 0.05$, ANOVA).